Acta Cryst E CRYSTALLOGRAPHIC COMMUNICATIONS

ISSN 2056-9890

Intermolecular interactions in a phenol-substituted benzimidazole

David K. Geiger,* H. Cristina Geiger and Shawn M. Moore

Department of Chemistry, SUNY-College at Geneseo, Geneseo, NY 14454, USA. *Correspondence e-mail: geiger@geneseo.edu

Received 22 January 2019
Accepted 23 January 2019

Edited by M. Zeller, Purdue University, USA

Keywords: crystal structure; hydrogen bonds; C—H···π interactions; Hirshfeld surface; density functional theory; interaction energy; benzimidazole.

CCDC reference: 1893078

Supporting information: this article has supporting information at journals.iucr.org/e

Hydrogen bonding plays an important role in the design of solid-state structures and gels with desirable properties. 1-(4-Hydroxybenzyl)-2-(4-hydroxyphenyl)-5,6-dimethyl-1*H*-benzimidazole was isolated as the acetone disolvate, $C_{22}H_{20}N_2O_2\cdot 2C_3H_6O$. O—H···N hydrogen bonding between benzimidazole molecules results in chains parallel to [010]. One of the acetone solvate molecules participates in O—H···O hydrogen bonding with the benzimidazole derivative. C—H···π interactions are observed in the extended structure. Hirshfeld surface analysis was used to explore the intermolecular interactions and density functional theory was used to estimate the strength of the hydrogen bonds.

1. Chemical context

The formation of a gel rather than a crystalline solid depends on the ability of the dissolved gelator to self-assemble into a three-dimensional network structure incorporating the solvent *via* non-covalent interactions rather than self-assembly followed by crystallization. The study of the gelation properties of small organic compounds (organogelators) is of importance in soft-matter research because of possible biomedical applications (Lau & Kiick, 2015; Huynh *et al.*, 2011; Ye *et al.*, 2014), including potential use in tissue engineering (Xavier *et al.*, 2015; Yan *et al.*, 2015), drug delivery and diagnostics (Wu & Wang, 2016; Tibbitt *et al.*, 2016), and medical implants (Liow *et al.*, 2016; Yasmeen *et al.*, 2014).

Our efforts in this area include the preparation, structural characterization and exploration of the intermolecular interactions in long-chain ester-substituted biphenyl derivatives (Geiger, Geiger, Moore *et al.*, 2017; Geiger, Geiger, Roberts *et al.*, 2018) and phenyphenol derivatives (Geiger, Geiger & Morell, 2018). We have also reported a novel long-chain ester-substituted benzimidazole gelator (Geiger, Zick *et al.*, 2017).

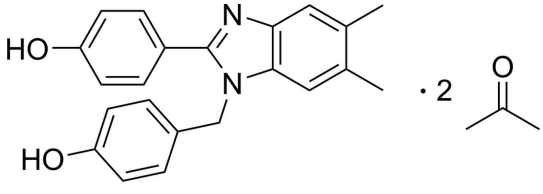

In our continuing efforts to exploit benzimidazole as a gelator core, we synthesized 1-(4-hydroxybenzyl)-2-(4-hydroxyphenyl)-5,6-dimethyl-1*H*-benzimidazole in the hope of using it as a starting material to prepare derivatives with a propensity for gelation. This compound was isolated as the diacetone solvate, (1), and we report herein its structural char-

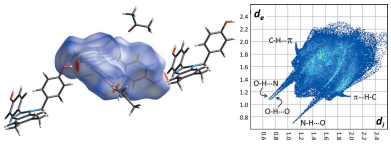

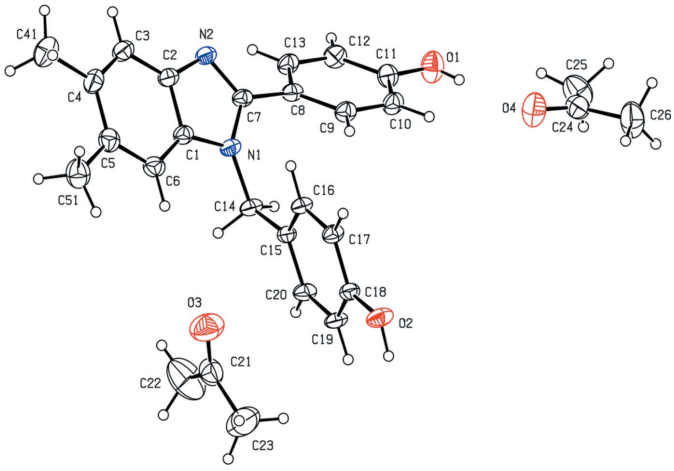

Figure 1
View of the molecular structure of (1) showing the atom-labeling scheme. Displacement ellipsoids for non-hydrogen atoms are drawn at the 30% probability level.

acterization and an exploration of its three-dimensional superstructure, including an examination of hydrogen-bond strengths.

2. Structural commentary

A view of the molecular structure of (1) with the atom-labeling scheme employed is seen in Fig. 1. The bond lengths and angles are all within the range reported for similar disubstituted benzimidazole derivatives (*c.f.* Geiger & DeStefano, 2016). The benzimidazole moiety is planar with the largest deviation for C7 [0.0344 (13) Å]. The 2-(4-hydroxyphenyl) substituent is canted at an angle of 44.18 (7)° from the benzimidazole plane and the N2—C7—C8—C13 torsion angle is −43.7 (2)°.

In addition to the benzimidazole, the asymmetric unit of (1) contains two acetone molecules, one of which uses its carbonyl oxygen atom as acceptor in an O—H···O hydrogen bond (see Table 1). The hydrogen-bonded acetone molecule exhibits a slightly longer C—O bond distance than the other acetone molecule [1.212 (3) Å *versus* 1.192 (3) Å]. This observation is consistent with previous results (Ichikawa, 1979).

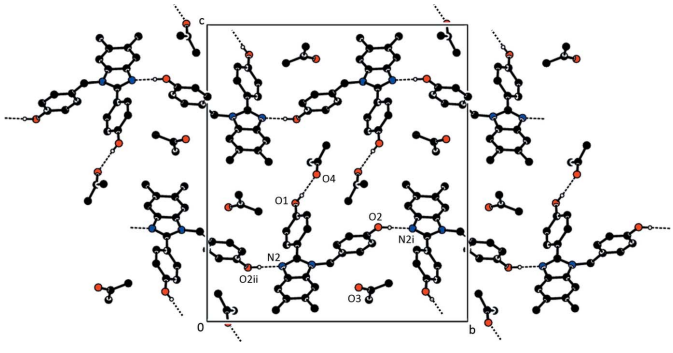

Figure 2
Partial packing diagram of (1) showing the O—H···N hydrogen bonding resulting in chains along [010]. Only H atoms involved in the interactions are shown. Symmetry codes: (i) $-x+2, y+\frac{1}{2}, -z+\frac{1}{2}$; (ii) $-x+2, y-\frac{1}{2}, -z+\frac{1}{2}$.

Table 1
Hydrogen-bond geometry (Å, °).

*Cg*3 is ring centroid of the 2-(4-hydroxyphenyl) substituent. *Cg*2 is ring centroid of the benzene ring of the benzimidazole ring system.

D—H···*A*	*D*—H	H···*A*	*D*···*A*	*D*—H···*A*
O1—H1···O4	0.81 (4)	1.96 (4)	2.748 (3)	165 (4)
O2—H2···N2^{i}	0.93 (3)	1.83 (3)	2.757 (2)	176 (2)
C16—H16···*Cg*3^{ii}	0.95	2.76	3.6061 (19)	149
C13—H13···*Cg*2^{iii}	0.95	3.00	3.552 (2)	119

Symmetry codes: (i) $-x+2, y+\frac{1}{2}, -z+\frac{1}{2}$; (ii) $x+1, y, z$; (iii) $x-1, y, z$.

3. Supramolecular features

Fig. 2 and Table 1 show the hydrogen-bonding network exhibited by (1). Each of the phenol groups behaves as a donor in a hydrogen bond. The 2-(4-hydroxyphenyl) substituent participates in an O—H···O interaction with one of the acetone solvate molecules as the acceptor. The 1-(4-hydroxyphenyl)methyl substituent forms an O—H···N hydrogen bond in which an adjacent benzimidazole moiety serves as the acceptor. The result is a chain structure that runs parallel to [010].

Fig. 3 shows the Hirshfeld surface and fingerprint plot for the disubstituted benzimidazole moiety. The prinicpal hydrogen-bonding interactions are clearly visible. The surface coverages corresponding to H···O and H···N interactions are 16.0% and 5.9%, respectively. There are no significant π–π interactions observed. The fingerprint plot does, however, reveal a weak C—H···π interaction that involves C16—H16 with the 2-(4-hydroxyphenyl) substituent ring system and C13—H13 with the benzene ring of the benzimidazole moiety (see Table 1 and Fig. 4). These interactions are between molecules translated along the *a* axis. The surface coverage corresponding to H···C interactions is 24.7%.

The interaction energies were calculated using density functional theory with the CE-B3LYP/6-31G(*d*,*p*) functional/basis set combination (see Section 7 for details). The results of the calculations are reported in Table 2. As expected, the electrostatic component is the primary contributor to the traditional hydrogen-bonding interactions and the dispersive

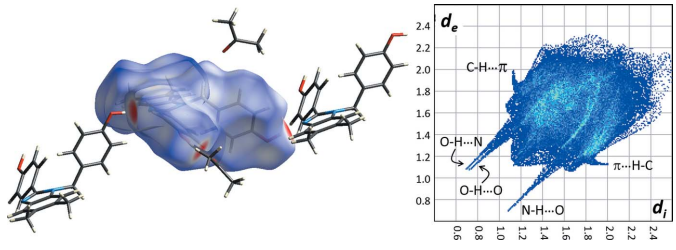

Figure 3
Hirshfeld surface (left) and fingerprint plot (right) for the benzimidazole moiety of (1).

Table 2
Interaction energies calculated for (1).

Energies are in kJ mol^{-1} and are corrected for BSSE.

Interaction	E'_{ele}	E'_{pol}	E'_{dis}	E'_{rep}	$E_{tot}^{1,2}$	E^3
O—H···N	−73.0	−19.9	−20.2	82	−58.8	−39.2
O—H···O	−48.9	−11.0	−9.0	50.1	−36.7	−35.7
C—H···π	−15.1	−4.5	−90.5	56.1	−63.5	−48.5

Notes: (i) Scale factors used to determine E_{tot}: k_{ele} = 1.057, k_{pol} = 0.740, $k_{energy\text{-}dispersive}$ = 0.871, k_{rep} = 0.618 (Mackenzie *et al.*, 2017). See Section 7 for calculation details. (ii) Interaction energies were calculated employing the CE-B3LYP/6–31G(*d,p*) functional/basis set combination. (iii) Interaction energies were calculated employing the M06–2X/6–31G(*d,p*) functional/basis set combination.

component dominates for the C—H···π interactions. The C—H···π interactions appear to reinforce each other with the sum of their contributions exceeding that of the traditional hydrogen-bond energies.

The M06 suite of density functionals are reported to outperform B3LYP for dispersion and ionic hydrogen-bonding interactions (Walker *et al.*, 2013; Zhao & Truhlar, 2008) and so the M06-2X/6-31G(*d,p*) functional/basis set combination was also used to calculate the interaction energies. The results are found in Table 2. The value obtained using the M06-2X functional compares favorably with the CE-B3LYP functional result for the phenol···acetone hydrogen bond, but the values are decidedly less for the C—H···π and the inter-benzimidazole O—H···N hydrogen bonds. The calculations employing the M06-2X functional were performed in the gas phase; however, in the solid state, intermolecular interactions do not occur in isolation, which may account for the difference in results.

O—H···O hydrogen bonds exhibit a large range of energies. For example, reported *o*-hydryoxy ketones have intramolecular hydrogen-bond strengths of −26.8 to −54.8 kJ mol^{-1} (Rusiniska-Roszak, 2017) and a series of CX[4} and CX[5] calixarenes have calculated O—H···O energies ranging from −19.2 to −34.4 kJ mol^{-1} (Khedkar *et al.*, 2012). The O—H···O hydrogen-bond energies in cyclodextrin conformers were found to range from −4.6 to −34.7 kJ mol^{-1} (Deshmukh *et al.*, 2011). As a final example, the hydrogen-bond energy in the optimized water dimer is −21 kJ mol^{-1} and in the hexamer water cluster it is −42 kJ mol^{-1} (Wendler *et al.*, 2010). The value obtained in the present study (Table 2) is comparable to these values.

The O—H···N hydrogen-bond strength is greater than the O—H···O hydrogen-bond strength in this example (Table 2), as has been observed for H_3SiOH with O- and N-atom acceptors (Beckmann & Grabowsky, 2007). For comparison, the intramolecular O—H···N hydrogen-bond strengths for a series of 2-hydroxybenzaldimine compounds range from −55 to −80 kJ mol^{-1}, depending on the imine substituent (Simperler & Mikenda, 1997); and the interaction energy for pyridine and formic acid is −46.4 kJ mol^{-1} (Fernandez-Berridi *et al.*, 2002).

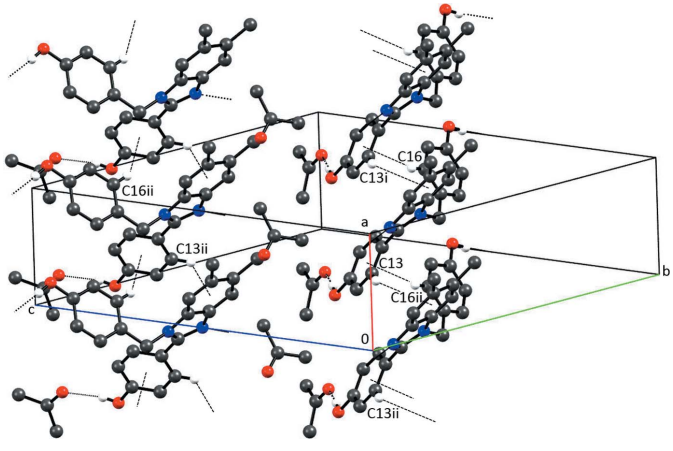

Figure 4
Partial packing diagram of (1) showing the chains along [100] resulting from C—H···π interactions. Only H atoms involved in interactions are shown. Symmetry codes: (i) $x+1, y, z$; (ii) $x-1, y, z$; (iii) $x, -y+\frac{1}{2}, z+\frac{1}{2}$.

4. Database survey

In 3-[1-(3-hydroxybenzyl)-1*H*-benzimidazol-2-yl]phenol, the 3-hydroxyphenyl substituent forms a dihedral angle of 56.55 (3)° with the benzimidazole moiety (Eltayeb, Teoh, Fun *et al.*, 2009). The structure of 1-(2-hydroxybenzyl)-2-(2-hydroxyphenyl)-1*H*-benzimidazol-3-ium chloride displays a dihedral angle of 55.49 (9)° between the benzimidazole core and the 2-hydroxyphenyl substituent (Khan *et al.*, 2017). 2-(1*H*-Benzimidazol-2-yl)phenol is essentially planar and exhibits an intramolecular hydrogen bond (Prakash *et al.*, 2014). In the hydrochloride salt of 2-(4-hydroxyphenyl)-1*H*-benzimidazole, the hydroxyphenyl substituent is essentially coplanar with the benzimidazole moiety (González-Padilla *et al.*, 2013). Other benzimidazole derivatives that have hydroxyphenyl substituents include 2-{[2-(pyridin-4-yl)-1*H*-benzimidazol-1-yl]methyl}phenol (Omer *et al.*, 2013), 2-[(1*H*-benzimidazol-1-yl)methyl]phenol benzene hemisolvate (Rivera *et al.*, 2014), 2-(1-phenyl-1*H*-benzimidazol-2-yl)phenol (Thiruvalluvar *et al.*, 2013), and 2-methoxy-6-(6-methyl-1*H*-benzimidazol-2-yl)phenol (Eltayeb, Teoh, Quah *et al.*, 2009).

5. Synthesis and crystallization

5,6-Dimethyl-2-(4-hydroxyphenyl)-1-[(4-hydroxyphenyl)-methyl]-1*H*-benzimidazole: 1.96 g (14.37 mmol) of 4,5-dimethyl-1,2-diaminobenzene were dissolved in 50 mL of ethanol and stirred under nitrogen. 3.65 g (29.9 mmol) of 4-hydroxybenzaldehyde were dissolved in ethanol, purged with nitrogen for 5 min., and then added dropwise to the solution. The solution was refluxed for 24 h and cooled, after which a yellow solid formed. This solid was filtered and washed with cold ethanol. 4.23 g (12.3 mmol, 85.5% yield) of the yellow solid was obtained. R_f (3:1 acetone/hexane) = 0.64. ^{1}H NMR (400MHz, DMSO): δ 2.23 ppm (*s*, 3H), δ 2.28 ppm (*s*, 3H), δ 5.33 ppm (*s*, 2H), δ 6.64 ppm (*d*, 2H), δ 6.78 ppm (*d*, 2H), δ 6.85 ppm (*d*, 2H), δ 7.15 ppm (*s*, 1H) δ 7.40 ppm (*s*, 1H), δ 7.50 ppm (*d*, 2H), δ 9.34 ppm (*s*, 1H), δ 9.88 ppm (*s*, 1H).

Table 3
Experimental details.

Crystal data	
Chemical formula	$C_{22}H_{20}N_2O_2{\cdot}2C_3H_6O$
M_r	460.55
Crystal system, space group	Monoclinic, $P2_1/c$
Temperature (K)	200
a, b, c (Å)	5.7307 (6), 19.733 (2), 22.436 (3)
β (°)	92.400 (4)
V (Å^3)	2534.9 (5)
Z	4
Radiation type	Mo $K\alpha$
μ (mm^{-1})	0.08
Crystal size (mm)	0.60 × 0.30 × 0.30
Data collection	
Diffractometer	Bruker SMART X2S benchtop
Absorption correction	Multi-scan (*SADABS*; Bruker, 2015)
T_{min}, T_{max}	0.35, 0.98
No. of measured, independent and observed [$I > 2\sigma(I)$] reflections	26416, 4489, 3268
R_{int}	0.093
(sin $\theta/\lambda)_{max}$ (Å^{-1})	0.596
Refinement	
$R[F^2 > 2\sigma(F^2)]$, $wR(F^2)$, S	0.058, 0.195, 1.07
No. of reflections	4489
No. of parameters	322
H-atom treatment	H atoms treated by a mixture of independent and constrained refinement
$\Delta\rho_{max}$, $\Delta\rho_{min}$ (e Å^{-3})	0.28, −0.29

Computer programs: *APEX2* and *SAINT* (Bruker, 2015), *SHELXS97* (Sheldrick, 2008), *SHELXL2014/7* (Sheldrick, 2015), *PLATON* (Spek, 2009), *Mercury* (Macrae *et al.*, 2008) and *publCIF* (Westrip, 2010).

Single crystals of (1) were obtained by slow evaporation of a dilute acetone solution of the product.

6. Refinement

Crystal data, data collection and structure refinement details are summarized in Table 3. A refined extinction coefficient [0.006 (2)] was employed to calculate the correction factor applied to the structure-factor data. H atoms bonded to C were refined using a riding model with C—H = 0.95 Å for H bonded to aromatic C atoms, 0.99 Å for methylene H atoms, and 0.98 Å for the methyl H atoms. U_{iso}(H) = kU_{eq}(C), where k = 1.2 for H atoms bonded to aromatic and methylene C atoms and 1.5 for H atoms bonded to methyl C atoms. H atoms bonded to oxygen were refined freely, including isotropic displacement parameters.

7. Hirshfeld surface, fingerprint plots, interaction energy calculations

Hirshfeld surfaces, fingerprint plots, and interaction energies were calculated using *CrystalExplorer17* (Turner *et al.*, 2017), in which the C—H bond lengths were converted to normalized values based on neutron diffraction results (Allen *et al.*, 2004). Interaction energies were calculated employing the CE-B3LYP/6-31G(*d,p*) functional/basis set combination and are corrected for basis set superposition energy (BSSE) using the counterpoise (CP) method (Boys & Bernardi, 1970). The interaction energy is broken down as

$$E_{tot} = k_{ele}E'_{ele} + k_{pol}E'_{pol} + k_{dis}E'_{dis} + k_{rep}E'_{rep}$$

where the k values are scale factors, E'_{ele} represents the electrostatic component, E'_{pol} the polarization energy, E'_{dis} the dispersion energy, and E'_{rep} the exchange-repulsion energy (Turner *et al.*, 2014; Mackenzie *et al.*, 2017).

Interaction energy calculations were also performed on molecules in the gas phase using *SPARTAN'16* (Wavefunction, 2016). DFT calculations using the M06-2X (Zhao & Truhlar, 2008) functional with a 6-31G(*d,p*) basis set were employed for the determination of interaction energies, which were corrected for BSSE employing the CP method (Boys & Bernardi, 1970). Atomic coordinates obtained from the crystallographic analysis were used for all non-H atoms. Because bond lengths obtained for H atoms from X-ray crystallographic analyses are unreliable, the positions of the H atoms were optimized to their energy minima using the M06-2X/6-31G(*d,p*) functional/basis set combination.

Funding information

This work was supported by a Congressionally directed grant from the US Department of Education for the X-ray diffractometer (award No. P116Z100020) and a grant from the Geneseo Foundation.

References

Allen, F. H., Watson, D. G., Brammer, L., Orpen, A. G. & Taylor, R. (2004). *International Tables for Crystallography*, 3rd ed., edited by E. Prince, pp. 790–811. Heidelberg: Springer Verlag.

Beckmann, J. & Grabowsky, S. (2007). *J. Phys. Chem. A*, **111**, 2011–2019.

Boys, S. F. & Bernardi, F. (1970). *Mol. Phys.* **19**, 553–566.

Bruker (2015). *APEX2*, *SAINT* and *SADABS*. Bruker AXS Inc., Madison, Wisconsin, USA.

Deshmukh, M. M., Bartolotti, L. J. & Gadre, S. (2011). *J. Comput. Chem.* **32**, 2996–3004.

Eltayeb, N. E., Teoh, S. G., Fun, H.-K., Jebas, S. R. & Adnan, R. (2009). *Acta Cryst.* E**65**, o1374–o1375.

Eltayeb, N. E., Teoh, S. G., Quah, C. K., Fun, H.-K. & Adnan, R. (2009). *Acta Cryst.* E**65**, o1613–o1614.

Fernandez-Berridi, M. J., Iruin, J. J., Irusta, L., Mercero, J. M. & Ugalde, J. M. (2002). *J. Phys. Chem. A*, **106**, 4187–4191.

Geiger, D. K. & DeStefano, M. R. (2016). *Acta Cryst.* C**72**, 867–874.

Geiger, D. K., Geiger, H. C., Moore, S. M. & Roberts, W. R. (2017). *Acta Cryst.* C**73**, 791–796.

Geiger, D. K., Geiger, H. C. & Morell, D. L. (2018). *Acta Cryst.* E**74**, 594–599.

Geiger, H. C., Geiger, D. K., Roberts, W. R., Morell, D. L., Huttunen, P., Schulman, J. L., Tran, M. & Farthing, D. (2018). *Gels*, **4**, 34–49.

Geiger, H. C., Zick, P. L., Roberts, W. R. & Geiger, D. K. (2017). *Acta Cryst.* C**73**, 350–356.

González-Padilla, J. E., Rosales-Hernández, M. C., Padilla-Martínez, I. I., García-Báez, E. V. & Rojas-Lima, S. (2013). *Acta Cryst.* E**69**, o1485–o1486.

Huynh, C. T., Nguyen, M. K. & Lee, D. S. (2011). *Macromolecules*, **44**, 6629–6636.

Ichikawa, M. (1979). *J. Cryst. Mol. Struct.* **9**, 87–105.

Khan, T., Mishra, N., Mhatre, D. S. & Datta, A. (2017). *Acta Cryst.* E**73**, 1143–1147.

Khedkar, J. K., Deshmukh, M. M., Gadre, S. R. & Gejji, S. P. (2012). *J. Phys. Chem. A*, **116**, 3739–3744.
Lau, H. K. & Kiick, K. L. (2015). *Biomacromolecules*, **16**, 28–42.
Liow, S. S., Dou, Q., Kai, D., Karim, A. A., Zhang, K., Xu, F. & Loh, X. J. (2016). *ACS Biomater. Sci. Eng.* **2**, 295–316.
Mackenzie, C. F., Spackman, P. R., Jayatilaka, D. & Spackman, M. A. (2017). *IUCrJ*, **4**, 575–587.
Macrae, C. F., Bruno, I. J., Chisholm, J. A., Edgington, P. R., McCabe, P., Pidcock, E., Rodriguez-Monge, L., Taylor, R., van de Streek, J. & Wood, P. A. (2008). *J. Appl. Cryst.* **41**, 466–470.
Omer, M. A. S., Liu, J. & Xiao, C. (2013). *Acta Cryst.* E**69**, o700.
Prakash, S. M., Thiruvalluvar, A., Rosepriya, S. & Srinivasan, N. (2014). *Acta Cryst.* E**70**, o184.
Rivera, A., Jiménez-Cruz, L. & Bolte, M. (2014). *Acta Cryst.* E**70**, o177.
Rusiniska-Roszak, D. (2017). *Molecules*, **22**, 481–581.
Sheldrick, G. M. (2008). *Acta Cryst.* A**64**, 112–122.
Sheldrick, G. M. (2015). *Acta Cryst.* A**71**, 3–8.
Simperler, A. & Mikenda, W. (1997). *Monatshefte für Chemie* **128**, 969–980.
Spek, A. L. (2009). *Acta Cryst.* D**65**, 148–155.
Thiruvalluvar, A., Rosepriya, S., Jayamoorthy, K., Jayabharathi, J., Öztürk Yildirim, S. & Butcher, R. J. (2013). *Acta Cryst.* E**69**, o62.
Tibbitt, M. W., Dahlman, J. E. & Langer, R. (2016). *J. Am. Chem. Soc.* **138**, 704–717.
Turner, M. J., Grabowsky, S., Jayatilaka, D. & Spackman, M. A. (2014). *J. Phys. Chem. Lett.* **5**, 4249–4255.
Turner, M. J., McKinnon, J. J., Wolff, S. K., Grimwood, D. J., Spackman, P. R., Jayatilaka, D. & Spackman, M. A. (2017). *CrystalExplorer17. University of Western Australia.* http://crystalexplorer.scb.uwa.edu.au
Walker, M., Harvey, A. J. A., Sen, A. & Dessent, C. E. H. (2013). *J. Phys. Chem. A*, **117**, 12590–12600.
Wavefunction. (2016). *SPARTAN'16*. Wavefunction Inc. Irvine, CA, USA.
Wendler, K., Thar, J., Zahn, S. & Kirchner, B. (2010). *J. Phys. Chem. A*, **114**, 9529–9536.
Westrip, S. P. (2010). *J. Appl. Cryst.* **43**, 920–925.
Wu, H.-Q. & Wang, C.-C. (2016). *Langmuir*, **32**, 6211–6225.
Xavier, J. R., Thakur, T., Desai, P., Jaiswal, M. K., Sears, N., Cosgriff-Hernandez, E., Kaunas, R. & Gaharwar, A. K. (2015). *ACS Nano*, **9**, 3109–3118.
Yan, L.-P., Oliveira, J. M., Oliveira, A. L. & Reis, R. L. (2015). *ACS Biomater. Sci. Eng.* **1**, 183–200.
Yasmeen, S., Lo, M. K., Bajracharya, S. & Roldo, M. (2014). *Langmuir*, **30**, 12977–12985.
Ye, E., Chee, P. L., Prasad, A., Fang, X., Owh, C., Yeo, V. J. J. & Loh, X. J. (2014). *Mater. Today*, **17**, 194–202.
Zhao, Y. & Truhlar, D. G. (2008). *Theor. Chem. Acc.* **120**, 215–241.

supporting information

Acta Cryst. (2019). E**75**, 272-276 [https://doi.org/10.1107/S2056989019001270]

Intermolecular interactions in a phenol-substituted benzimidazole

David K. Geiger, H. Cristina Geiger and Shawn M. Moore

Computing details

Data collection: *APEX2* (Bruker, 2015); cell refinement: *SAINT* (Bruker, 2015); data reduction: *SAINT* (Bruker, 2015); program(s) used to solve structure: *SHELXS97* (Sheldrick, 2008); program(s) used to refine structure: *SHELXL2014/7* (Sheldrick, 2015); molecular graphics: *PLATON* (Spek, 2009), *Mercury* (Macrae *et al.*, 2008); software used to prepare material for publication: *publCIF* (Westrip, 2010).

1-(4-Hydroxybenzyl)-2-(4-hydroxyphenyl)-5,6-dimethyl-1*H*-benzimidazole acetone disolvate

Crystal data

$C_{22}H_{20}N_2O_2\cdot 2C_3H_6O$
$M_r = 460.55$
Monoclinic, $P2_1/c$
$a = 5.7307$ (6) Å
$b = 19.733$ (2) Å
$c = 22.436$ (3) Å
$\beta = 92.400$ (4)°
$V = 2534.9$ (5) Å^3
$Z = 4$
$F(000) = 984$
$D_x = 1.207$ Mg m^{-3}
Mo $K\alpha$ radiation, $\lambda = 0.71073$ Å
Cell parameters from 7680 reflections
$\theta = 2.3$–25.0°
$\mu = 0.08$ mm^{-1}
$T = 200$ K
Prism, clear colourless
0.60 × 0.30 × 0.30 mm

Data collection

Bruker SMART X2S benchtop diffractometer
Radiation source: XOS X-beam microfocus source
Doubly curved silicon crystal monochromator
Detector resolution: 8.3330 pixels mm^{-1}
ω scans
Absorption correction: multi-scan (SADABS; Bruker, 2015)
$T_{min} = 0.35$, $T_{max} = 0.98$
26416 measured reflections
4489 independent reflections
3268 reflections with $I > 2\sigma(I)$
$R_{int} = 0.093$
$\theta_{max} = 25.1°$, $\theta_{min} = 2.1°$
$h = -6\rightarrow 6$
$k = -22\rightarrow 23$
$l = -26\rightarrow 26$

Refinement

Refinement on F^2
Least-squares matrix: full
$R[F^2 > 2\sigma(F^2)] = 0.058$
$wR(F^2) = 0.195$
$S = 1.07$
4489 reflections
322 parameters
0 restraints
Primary atom site location: structure-invariant direct methods
Secondary atom site location: difference Fourier map
Hydrogen site location: mixed
H atoms treated by a mixture of independent and constrained refinement
$w = 1/[\sigma^2(F_o^2) + (0.124P)^2]$ where $P = (F_o^2 + 2F_c^2)/3$
$(\Delta/\sigma)_{max} = 0.001$
$\Delta\rho_{max} = 0.28$ e Å^{-3}
$\Delta\rho_{min} = -0.28$ e Å^{-3}
Extinction correction: SHELXL-2014/7 (Sheldrick 2015)
Extinction coefficient: 0.006 (2)

Special details

Geometry. All esds (except the esd in the dihedral angle between two l.s. planes) are estimated using the full covariance matrix. The cell esds are taken into account individually in the estimation of esds in distances, angles and torsion angles; correlations between esds in cell parameters are only used when they are defined by crystal symmetry. An approximate (isotropic) treatment of cell esds is used for estimating esds involving l.s. planes.

Refinement. Refinement of F^2 against ALL reflections. The weighted R-factor wR and goodness of fit S are based on F^2, conventional R-factors R are based on F, with F set to zero for negative F^2. The threshold expression of $F^2 > 2\text{sigma}(F^2)$ is used only for calculating R-factors(gt) etc. and is not relevant to the choice of reflections for refinement. R-factors based on F^2 are statistically about twice as large as those based on F, and R- factors based on ALL data will be even larger.

Fractional atomic coordinates and isotropic or equivalent isotropic displacement parameters (Å²)

	x	*y*	*z*	U_{iso}*/U_{eq}
O1	0.0984 (3)	0.33911 (10)	0.39918 (10)	0.0665 (6)
H1	0.154 (7)	0.3632 (18)	0.425 (2)	0.110 (14)*
O2	1.3625 (3)	0.65683 (6)	0.31799 (8)	0.0513 (5)
H2	1.304 (5)	0.7006 (14)	0.3166 (12)	0.066 (7)*
O3	0.3839 (4)	0.58204 (10)	0.11484 (12)	0.0973 (8)
O4	0.2047 (4)	0.42019 (11)	0.49612 (10)	0.0795 (6)
N1	0.8301 (3)	0.40174 (7)	0.19126 (8)	0.0357 (5)
N2	0.7935 (3)	0.28900 (7)	0.18639 (8)	0.0378 (5)
C1	0.9855 (3)	0.37992 (8)	0.14968 (10)	0.0367 (5)
C2	0.9600 (3)	0.30963 (8)	0.14685 (10)	0.0379 (5)
C3	1.1005 (4)	0.27223 (9)	0.11001 (11)	0.0459 (6)
H3	1.0836	0.2244	0.1076	0.055*
C4	1.2651 (4)	0.30477 (11)	0.07677 (11)	0.0487 (6)
C5	1.2878 (4)	0.37676 (10)	0.07961 (11)	0.0469 (6)
C6	1.1473 (4)	0.41409 (9)	0.11616 (10)	0.0435 (6)
H6	1.161	0.462	0.1183	0.052*
C7	0.7220 (3)	0.34487 (8)	0.21232 (10)	0.0341 (5)
C8	0.5588 (3)	0.34613 (8)	0.26094 (10)	0.0362 (5)
C9	0.6028 (4)	0.38479 (9)	0.31208 (11)	0.0405 (6)
H9	0.7375	0.4129	0.3149	0.049*
C10	0.4532 (4)	0.38297 (9)	0.35902 (11)	0.0446 (6)
H10	0.4866	0.4093	0.3938	0.054*
C11	0.2546 (4)	0.34270 (10)	0.35521 (11)	0.0444 (6)
C12	0.2085 (4)	0.30419 (10)	0.30451 (11)	0.0474 (6)
H12	0.0719	0.2769	0.3015	0.057*
C13	0.3607 (4)	0.30533 (9)	0.25829 (10)	0.0409 (6)
H13	0.3294	0.2778	0.2242	0.049*
C14	0.7491 (3)	0.47223 (8)	0.19678 (10)	0.0387 (5)
H14A	0.5982	0.4719	0.2167	0.046*
H14B	0.7199	0.4909	0.1562	0.046*
C15	0.9149 (3)	0.51921 (8)	0.23098 (9)	0.0326 (5)
C16	1.1243 (3)	0.49868 (8)	0.25815 (10)	0.0367 (5)
H16	1.1679	0.4523	0.257	0.044*
C17	1.2716 (3)	0.54515 (8)	0.28710 (10)	0.0378 (5)
H17	1.4148	0.5302	0.3055	0.045*

C18	1.2115 (4)	0.61319 (8)	0.28943 (10)	0.0359 (5)
C19	0.9987 (4)	0.63368 (8)	0.26372 (10)	0.0414 (6)
H19	0.953	0.6798	0.266	0.05*
C20	0.8527 (3)	0.58733 (9)	0.23476 (10)	0.0405 (6)
H20	0.7079	0.6021	0.2172	0.049*
C21	0.2570 (5)	0.62914 (14)	0.10570 (13)	0.0626 (7)
C22	0.0308 (7)	0.6214 (2)	0.0731 (2)	0.1300 (18)
H22A	0.0203	0.5759	0.0555	0.195*
H22B	0.0169	0.6554	0.0413	0.195*
H22C	−0.0957	0.6276	0.1006	0.195*
C23	0.3276 (7)	0.69718 (15)	0.1289 (2)	0.1050 (13)
H23A	0.2746	0.7026	0.1696	0.158*
H23B	0.2566	0.7324	0.1032	0.158*
H23C	0.4981	0.7013	0.1292	0.158*
C24	0.0807 (5)	0.42468 (12)	0.53839 (13)	0.0580 (7)
C25	−0.1601 (5)	0.39762 (17)	0.53648 (16)	0.0822 (10)
H25A	−0.2715	0.4351	0.5316	0.123*
H25B	−0.1877	0.3736	0.5738	0.123*
H25C	−0.1808	0.3662	0.5028	0.123*
C26	0.1701 (7)	0.45779 (19)	0.59377 (15)	0.0916 (11)
H26A	0.3078	0.485	0.5853	0.137*
H26B	0.2131	0.4231	0.6235	0.137*
H26C	0.0488	0.4872	0.6092	0.137*
C41	1.4225 (5)	0.26394 (14)	0.03844 (15)	0.0718 (8)
H41A	1.3985	0.2155	0.0458	0.108*
H41B	1.5858	0.2757	0.0483	0.108*
H41C	1.3858	0.274	−0.0037	0.108*
C51	1.4674 (5)	0.41265 (14)	0.04431 (13)	0.0649 (7)
H51A	1.4655	0.4612	0.0537	0.097*
H51B	1.4314	0.4062	0.0016	0.097*
H51C	1.6224	0.394	0.0546	0.097*

Atomic displacement parameters (Å²)

	U^{11}	U^{22}	U^{33}	U^{12}	U^{13}	U^{23}
O1	0.0602 (12)	0.0842 (12)	0.0556 (13)	−0.0163 (9)	0.0101 (10)	−0.0131 (10)
O2	0.0532 (10)	0.0285 (7)	0.0705 (12)	−0.0013 (6)	−0.0172 (9)	−0.0070 (6)
O3	0.1049 (17)	0.0705 (11)	0.114 (2)	0.0236 (12)	−0.0186 (15)	−0.0043 (13)
O4	0.0804 (14)	0.0976 (14)	0.0612 (15)	−0.0162 (11)	0.0109 (11)	−0.0186 (12)
N1	0.0392 (9)	0.0242 (7)	0.0432 (11)	0.0010 (6)	−0.0033 (8)	−0.0035 (7)
N2	0.0433 (10)	0.0270 (7)	0.0429 (11)	0.0003 (6)	−0.0030 (8)	−0.0021 (7)
C1	0.0390 (12)	0.0320 (8)	0.0386 (12)	0.0010 (8)	−0.0061 (10)	−0.0018 (8)
C2	0.0418 (12)	0.0298 (8)	0.0411 (13)	0.0024 (8)	−0.0089 (10)	−0.0020 (8)
C3	0.0534 (14)	0.0358 (9)	0.0476 (14)	0.0036 (9)	−0.0057 (11)	−0.0073 (9)
C4	0.0509 (13)	0.0519 (11)	0.0427 (14)	0.0081 (10)	−0.0043 (11)	−0.0119 (10)
C5	0.0464 (13)	0.0519 (11)	0.0416 (14)	−0.0005 (10)	−0.0055 (11)	−0.0007 (10)
C6	0.0481 (13)	0.0375 (9)	0.0443 (14)	−0.0036 (9)	−0.0049 (11)	0.0016 (9)
C7	0.0342 (11)	0.0282 (8)	0.0394 (12)	−0.0011 (7)	−0.0068 (9)	−0.0003 (8)

C8	0.0361 (11)	0.0286 (8)	0.0430 (13)	0.0008 (7)	−0.0076 (10)	0.0001 (8)
C9	0.0402 (12)	0.0356 (9)	0.0451 (14)	−0.0048 (8)	−0.0056 (10)	−0.0027 (9)
C10	0.0483 (13)	0.0413 (9)	0.0434 (14)	−0.0034 (9)	−0.0079 (11)	−0.0086 (9)
C11	0.0416 (12)	0.0499 (11)	0.0416 (13)	−0.0003 (9)	−0.0005 (10)	−0.0004 (10)
C12	0.0449 (13)	0.0449 (10)	0.0520 (15)	−0.0122 (9)	−0.0038 (12)	−0.0032 (10)
C13	0.0418 (12)	0.0354 (9)	0.0447 (13)	−0.0035 (8)	−0.0076 (10)	−0.0060 (9)
C14	0.0399 (11)	0.0242 (8)	0.0513 (14)	0.0044 (7)	−0.0073 (9)	−0.0029 (8)
C15	0.0370 (11)	0.0250 (8)	0.0358 (12)	0.0011 (7)	−0.0001 (9)	0.0004 (8)
C16	0.0405 (11)	0.0230 (7)	0.0463 (13)	0.0053 (7)	0.0001 (9)	−0.0016 (8)
C17	0.0364 (11)	0.0312 (8)	0.0455 (13)	0.0056 (7)	−0.0048 (9)	−0.0025 (8)
C18	0.0422 (11)	0.0252 (7)	0.0400 (12)	−0.0016 (7)	−0.0013 (9)	−0.0004 (8)
C19	0.0492 (12)	0.0216 (7)	0.0530 (14)	0.0060 (8)	−0.0034 (10)	−0.0011 (8)
C20	0.0400 (11)	0.0290 (8)	0.0518 (14)	0.0062 (7)	−0.0072 (10)	0.0025 (8)
C21	0.0641 (17)	0.0717 (15)	0.0526 (17)	0.0047 (13)	0.0095 (13)	0.0064 (13)
C22	0.094 (3)	0.183 (4)	0.110 (4)	−0.017 (3)	−0.031 (3)	0.046 (3)
C23	0.124 (3)	0.0691 (17)	0.124 (4)	0.0031 (19)	0.026 (3)	−0.017 (2)
C24	0.0678 (17)	0.0531 (12)	0.0526 (17)	−0.0043 (12)	−0.0010 (13)	0.0046 (12)
C25	0.071 (2)	0.100 (2)	0.075 (2)	−0.0180 (17)	−0.0023 (16)	0.0165 (18)
C26	0.112 (3)	0.108 (2)	0.056 (2)	−0.038 (2)	0.0110 (18)	−0.0129 (18)
C41	0.0707 (18)	0.0746 (16)	0.071 (2)	0.0101 (14)	0.0105 (15)	−0.0199 (15)
C51	0.0612 (16)	0.0765 (15)	0.0573 (18)	−0.0092 (13)	0.0066 (13)	−0.0028 (14)

Geometric parameters (Å, º)

O1—C11	1.361 (3)	C14—H14B	0.99
O1—H1	0.81 (4)	C15—C16	1.384 (2)
O2—C18	1.362 (2)	C15—C20	1.394 (2)
O2—H2	0.93 (3)	C16—C17	1.389 (2)
O3—C21	1.192 (3)	C16—H16	0.95
O4—C24	1.212 (3)	C17—C18	1.388 (2)
N1—C7	1.375 (2)	C17—H17	0.95
N1—C1	1.385 (3)	C18—C19	1.387 (3)
N1—C14	1.473 (2)	C19—C20	1.383 (3)
N2—C7	1.320 (2)	C19—H19	0.95
N2—C2	1.391 (3)	C20—H20	0.95
C1—C6	1.392 (3)	C21—C22	1.470 (4)
C1—C2	1.396 (2)	C21—C23	1.490 (4)
C2—C3	1.390 (3)	C22—H22A	0.98
C3—C4	1.385 (3)	C22—H22B	0.98
C3—H3	0.95	C22—H22C	0.98
C4—C5	1.428 (3)	C23—H23A	0.98
C4—C41	1.506 (4)	C23—H23B	0.98
C5—C6	1.385 (3)	C23—H23C	0.98
C5—C51	1.502 (4)	C24—C26	1.477 (4)
C6—H6	0.95	C24—C25	1.479 (4)
C7—C8	1.466 (3)	C25—H25A	0.98
C8—C13	1.391 (3)	C25—H25B	0.98
C8—C9	1.392 (3)	C25—H25C	0.98

C9—C10	1.386 (3)	C26—H26A	0.98
C9—H9	0.95	C26—H26B	0.98
C10—C11	1.388 (3)	C26—H26C	0.98
C10—H10	0.95	C41—H41A	0.98
C11—C12	1.384 (3)	C41—H41B	0.98
C12—C13	1.383 (3)	C41—H41C	0.98
C12—H12	0.95	C51—H51A	0.98
C13—H13	0.95	C51—H51B	0.98
C14—C15	1.513 (2)	C51—H51C	0.98
C14—H14A	0.99		

C11—O1—H1	104 (3)	C17—C16—H16	119.6
C18—O2—H2	110.6 (17)	C18—C17—C16	120.63 (16)
C7—N1—C1	106.82 (15)	C18—C17—H17	119.7
C7—N1—C14	126.42 (18)	C16—C17—H17	119.7
C1—N1—C14	124.31 (17)	O2—C18—C19	122.80 (15)
C7—N2—C2	105.70 (15)	O2—C18—C17	118.41 (16)
N1—C1—C6	132.44 (16)	C19—C18—C17	118.78 (16)
N1—C1—C2	105.69 (19)	C20—C19—C18	120.44 (15)
C6—C1—C2	121.8 (2)	C20—C19—H19	119.8
C3—C2—N2	130.84 (16)	C18—C19—H19	119.8
C3—C2—C1	119.5 (2)	C19—C20—C15	121.00 (16)
N2—C2—C1	109.58 (19)	C19—C20—H20	119.5
C4—C3—C2	119.92 (18)	C15—C20—H20	119.5
C4—C3—H3	120.0	O3—C21—C22	121.5 (3)
C2—C3—H3	120.0	O3—C21—C23	119.2 (3)
C3—C4—C5	120.0 (2)	C22—C21—C23	119.3 (3)
C3—C4—C41	119.8 (2)	C21—C22—H22A	109.5
C5—C4—C41	120.2 (2)	C21—C22—H22B	109.5
C6—C5—C4	120.1 (2)	H22A—C22—H22B	109.5
C6—C5—C51	119.3 (2)	C21—C22—H22C	109.5
C4—C5—C51	120.6 (2)	H22A—C22—H22C	109.5
C5—C6—C1	118.62 (18)	H22B—C22—H22C	109.5
C5—C6—H6	120.7	C21—C23—H23A	109.5
C1—C6—H6	120.7	C21—C23—H23B	109.5
N2—C7—N1	112.2 (2)	H23A—C23—H23B	109.5
N2—C7—C8	124.15 (16)	C21—C23—H23C	109.5
N1—C7—C8	123.52 (16)	H23A—C23—H23C	109.5
C13—C8—C9	118.1 (2)	H23B—C23—H23C	109.5
C13—C8—C7	120.22 (18)	O4—C24—C26	119.8 (3)
C9—C8—C7	121.54 (17)	O4—C24—C25	121.9 (3)
C10—C9—C8	121.03 (18)	C26—C24—C25	118.4 (3)
C10—C9—H9	119.5	C24—C25—H25A	109.5
C8—C9—H9	119.5	C24—C25—H25B	109.5
C9—C10—C11	120.0 (2)	H25A—C25—H25B	109.5
C9—C10—H10	120.0	C24—C25—H25C	109.5
C11—C10—H10	120.0	H25A—C25—H25C	109.5
O1—C11—C12	117.3 (2)	H25B—C25—H25C	109.5

O1—C11—C10	123.2 (2)	C24—C26—H26A	109.5
C12—C11—C10	119.5 (2)	C24—C26—H26B	109.5
C13—C12—C11	120.17 (19)	H26A—C26—H26B	109.5
C13—C12—H12	119.9	C24—C26—H26C	109.5
C11—C12—H12	119.9	H26A—C26—H26C	109.5
C12—C13—C8	121.11 (19)	H26B—C26—H26C	109.5
C12—C13—H13	119.4	C4—C41—H41A	109.5
C8—C13—H13	119.4	C4—C41—H41B	109.5
N1—C14—C15	115.33 (14)	H41A—C41—H41B	109.5
N1—C14—H14A	108.4	C4—C41—H41C	109.5
C15—C14—H14A	108.4	H41A—C41—H41C	109.5
N1—C14—H14B	108.4	H41B—C41—H41C	109.5
C15—C14—H14B	108.4	C5—C51—H51A	109.5
H14A—C14—H14B	107.5	C5—C51—H51B	109.5
C16—C15—C20	118.32 (15)	H51A—C51—H51B	109.5
C16—C15—C14	123.96 (14)	C5—C51—H51C	109.5
C20—C15—C14	117.72 (15)	H51A—C51—H51C	109.5
C15—C16—C17	120.78 (15)	H51B—C51—H51C	109.5
C15—C16—H16	119.6		

C7—N1—C1—C6	−176.90 (19)	N2—C7—C8—C13	−43.7 (2)
C14—N1—C1—C6	19.9 (3)	N1—C7—C8—C13	140.81 (17)
C7—N1—C1—C2	1.05 (18)	N2—C7—C8—C9	132.74 (18)
C14—N1—C1—C2	−162.14 (15)	N1—C7—C8—C9	−42.8 (2)
C7—N2—C2—C3	176.53 (19)	C13—C8—C9—C10	−0.2 (3)
C7—N2—C2—C1	−0.28 (19)	C7—C8—C9—C10	−176.75 (16)
N1—C1—C2—C3	−177.72 (16)	C8—C9—C10—C11	−0.7 (3)
C6—C1—C2—C3	0.5 (3)	C9—C10—C11—O1	−179.10 (19)
N1—C1—C2—N2	−0.49 (19)	C9—C10—C11—C12	0.5 (3)
C6—C1—C2—N2	177.73 (16)	O1—C11—C12—C13	−179.72 (19)
N2—C2—C3—C4	−176.16 (18)	C10—C11—C12—C13	0.7 (3)
C1—C2—C3—C4	0.4 (3)	C11—C12—C13—C8	−1.7 (3)
C2—C3—C4—C5	−1.0 (3)	C9—C8—C13—C12	1.4 (3)
C2—C3—C4—C41	178.0 (2)	C7—C8—C13—C12	177.96 (17)
C3—C4—C5—C6	0.8 (3)	C7—N1—C14—C15	119.1 (2)
C41—C4—C5—C6	−178.2 (2)	C1—N1—C14—C15	−81.0 (2)
C3—C4—C5—C51	179.3 (2)	N1—C14—C15—C16	−2.9 (3)
C41—C4—C5—C51	0.3 (3)	N1—C14—C15—C20	176.6 (2)
C4—C5—C6—C1	0.0 (3)	C20—C15—C16—C17	−1.7 (3)
C51—C5—C6—C1	−178.48 (19)	C14—C15—C16—C17	177.8 (2)
N1—C1—C6—C5	176.97 (19)	C15—C16—C17—C18	0.1 (4)
C2—C1—C6—C5	−0.7 (3)	C16—C17—C18—O2	−179.6 (2)
C2—N2—C7—N1	0.98 (19)	C16—C17—C18—C19	1.7 (4)
C2—N2—C7—C8	−174.96 (16)	O2—C18—C19—C20	179.4 (2)
C1—N1—C7—N2	−1.31 (19)	C17—C18—C19—C20	−1.9 (4)
C14—N1—C7—N2	161.42 (17)	C18—C19—C20—C15	0.3 (4)
C1—N1—C7—C8	174.66 (16)	C16—C15—C20—C19	1.5 (4)
C14—N1—C7—C8	−22.6 (3)	C14—C15—C20—C19	−178.0 (2)

Hydrogen-bond geometry (Å, º)

*Cg*3 is ring centroid of the 2-(4-hydroxyphenyl) substituent. *Cg*2 is ring centroid of the benzene ring of the benzimidazole ring system.

D—H···*A*	*D*—H	H···*A*	*D*···*A*	*D*—H···*A*
O1—H1···O4	0.81 (4)	1.96 (4)	2.748 (3)	165 (4)
O2—H2···N2^{i}	0.93 (3)	1.83 (3)	2.757 (2)	176 (2)
C16—H16···*Cg*3^{ii}	0.95	2.76	3.6061 (19)	149
C13—H13···*Cg*2^{iii}	0.95	3.00	3.552 (2)	119

Symmetry codes: (i) −*x*+2, *y*+1/2, −*z*+1/2; (ii) *x*+1, *y*, *z*; (iii) *x*−1, *y*, *z*.